Title
Post-Mount Pinatubo eruption ground-based infrared stratospheric column measurements of HNO3, NO, and NO2 and their comparison with model calculations

Journal
Journal of Geophysical Research, 108(D15)

ISSN
0148-0227

Authors
Rinsland, Curtis P
Weisenstein, DK
Ko, MKW
et al.

Publication Date
2003

DOI
10.1029/2002jd002965

JOURNAL OF GEOPHYSICAL RESEARCH, VOL. 108, NO. D15, 4437, doi:10.1029/2002JD002965, 2003

Post-Mount Pinatubo eruption ground-based infrared stratospheric column measurements of HNO_3, NO, and NO_2 and their comparison with model calculations

Curtis P. Rinsland,[1] D. K. Weisenstein,[2] M. K. W. Ko,[1] C. J. Scott,[2] L. S. Chiou,[3] E. Mahieu,[4] R. Zander,[4] and P. Demoulin[4]

Received 19 September 2002; revised 13 February 2003; accepted 24 March 2003; published 1 August 2003.

[1] Infrared solar spectra recorded between July 1991 to March 1992 and November 2002 with the Fourier transform spectrometer on Kitt Peak (31.9°N latitude, 111.6°W longitude, 2.09 km altitude) have been analyzed to retrieve stratospheric columns of HNO_3, NO, and NO_2. The measurements cover a decade time span following the June 1991 Mount Pinatubo volcanic eruption and were recorded typically at 0.01 cm^{-1} spectral resolution. The measured HNO_3 stratospheric column shows a 20% decline from 9.16×10^{15} molecules cm^{-2} from the first observation in March 1992 to 7.40×10^{15} molecules cm^{-2} at the start of 1996 reaching a broad minimum of 6.95×10^{15} molecules cm^{-2} thereafter. Normalized daytime NO and NO_2 stratospheric column trends for the full post-Pinatubo eruption time period equal (+1.56 ± 0.45)% yr^{-1}, 1 sigma, and (+0.52 ± 0.32)% yr^{-1}, 1 sigma, respectively. The long-term trends are superimposed on seasonal cycles with ~10% relative amplitudes with respect to mean values, winter maxima for HNO_3 and summer maxima for NO and NO_2. The measurements have been compared with two-dimensional model calculations utilizing version 6.1 Stratospheric Aerosol and Gas Experiment (SAGE) II sulfate aerosol surface area density measurements through 1999 and extended to the end of the time series by repeating the 1999 values. The model-calculated HNO_3, NO, and NO_2 stratospheric column time series agree with the measurements to within ~8% after taking into account the vertical sensitivity of the ground-based measurements. The consistency between the measured and model-calculated stratospheric time series confirms the decreased impact on stratospheric reactive nitrogen chemistry of the key heterogeneous reaction that converts reactive nitrogen to its less active reservoir form as the lower-stratospheric aerosol surface area density declined by a factor of ~20 after the eruption maximum. *INDEX TERMS:* 0325 Atmospheric Composition and Structure: Evolution of the atmosphere; 0340 Atmospheric Composition and Structure: Middle atmosphere—composition and chemistry; 0341 Atmospheric Composition and Structure: Middle atmosphere—constituent transport and chemistry (3334); 0370 Atmospheric Composition and Structure: Volcanic effects (8409); 0368 Atmospheric Composition and Structure: Troposphere—constituent transport and chemistry

Citation: Rinsland, C. P., D. K. Weisenstein, M. K. W. Ko, C. J. Scott, L. S. Chiou, E. Mahieu, R. Zander, and P. Demoulin, Post-Mount Pinatubo eruption ground-based infrared stratospheric column measurements of HNO_3, NO, and NO_2 and their comparison with model calculations, *J. Geophys. Res.*, *108*(D15), 4437, doi:10.1029/2002JD002965, 2003.

1. Introduction

[2] A key heterogeneous reaction on sulfuric acid aerosol surfaces converts dinitrogen pentoxide (N_2O_5) to nitric acid (HNO_3):

$$N_2O_5 + H_2O \rightarrow HNO_3 + HNO_3 \quad (1)$$

with the immediate result that NO_x ($NO + NO_2$) is decreased, and due to the coupling among the chlorine, nitrogen, and hydrogen families, the concentrations of reactive chlorine and HO_x ($OH + HO_2 + H_2O_2$) are predicted to increase [*Poole et al.*, 1992]. Laboratory measurements indicate reaction (1) is independent of temperature and very efficient over a wide range of sulfate aerosol water content [*Tolbert et al.*, 1988; *Hanson and Ravishankara*, 1991]. Model calculations predict reaction (1) modifies stratospheric chemistry even at background aerosol levels leading to significant reductions in the abundances of the reactive nitrogen species NO_2 [*Considine et al.*, 1992; *Brasseur and Granier*, 1992] and NO [*Rodriguez et al.*, 1991] and corresponding increases in HNO_3 and decreases in N_2O_5. The impact of reaction (1) on

[1]NASA Langley Research Center, Hampton, Virginia, USA.
[2]Atmospheric and Environmental Research, Inc., Lexington, Massachusetts, USA.
[3]Science Applications International Corporation, Hampton, Virginia, USA.
[4]Institute of Astrophysics and Geophysics, University of Liège, Liège, Belgium.

0148-0227/03/2002JD002965

reactive nitrogen chemistry and partitioning occurs primarily below 30 km altitude, but may extend to higher altitudes shortly after major volcanic eruptions that increase sulfate aerosol surface area loading.

[3] Previous analyses of data from balloon and aircraft campaigns showed discrepancies between observed and modeled NO_y partitioning ($NO_y = NO + NO_2 + NO_3 + HNO_3 + 2N_2O_5 + HNO_4 + ClONO_2 + BrONO$). The NO_x/NO_y values calculated with JPL-97 reaction rates [*DeMore et al.*, 1997] are on the order of 10–30% smaller than the observed values in the lower stratosphere [*Osterman et al.*, 1999; *Gao et al.*, 1999; *Jucks et al.*, 1999] and larger discrepancies existed above 30 km [*Jucks et al.*, 1999]. The discrepancies in the lower stratosphere were resolved with new kinetic data indicating a faster (compared to the JPL-97) rate for the reaction of OH with HNO_3 [*Brown et al.*, 1999a] and the reaction of OH with NO_2 [*Brown et al.*, 1999b]. These rates have been adopted in the JPL-00 recommendation [*Sander et al.*, 2000]. With these new data, reaction (1) continues to play an important role at background aerosol levels in the lower stratosphere. *Jucks et al.* [1999] discussed several possible ways to resolve the discrepancy in HNO_3 above 25 km. The effect of uncertainties at these altitudes on the column should be small.

[4] Following the large April 1983 eruption of El Chichón [*Hofmann and Solomon*, 1989] and the massive June 1991 Mount Pinatubo eruption [*Fahey et al.*, 1993; *Rinsland et al.*, 1994; *Koike et al.*, 1994; *David et al.*, 1994], large increases in sulfate aerosol loading perturbed lower stratospheric reactive nitrogen chemistry through reaction (1). Sulfate aerosol loading decayed exponentially during the first three years after the Mount Pinatubo eruption with a time constant of 1.0 ± 0.2 years primarily as a result of sedimentation [*Godin et al.*, 1999, section 3.3.1.2], and is now below background levels typical of the late 1980s ($\sim$0.9 μm^2 cm^{-3}) in the lower stratosphere.

[5] Analysis of 1980–1998 measurements above Lauder, New Zealand (45°S latitude, 169.7° longitude, 0.37 km altitude) from slant column sunrise and sunset measurements showed NO_2 total columns increased at a rate of about 5% per decade, twice the increase rate of surface N_2O [*Liley et al.*, 2000]. As N_2O is the sole significant source of stratospheric NO_2 (minor sources include galactic cosmic rays, solar proton events and solar electrons), the observed NO_2 trend above the station could not be simply explained. *Fish et al.* [2000] were unable to explain the observed trend as a result of chemical impacts due to changes in stratospheric temperatures, ozone concentrations, or water vapor. They concluded that the aerosol trend is likely to have played a significant role because of the high sensitivity of the NO_2 trend to aerosol loading. A 20% decrease in aerosol surface area per decade creates agreement between the measured and calculated NO_2 trend. More recently, *McLinden et al.* [2001] used a combination of a photochemical box and three-dimensional transport model to reinterpret the same Lauder NO_2 time series. They attributed only half of the NO_2 increase as directly due to the rise in N_2O at the surface, with the remainder of the NO_2 rise caused by ozone changes, the impact of increased halogens on odd-nitrogen partitioning, and changes in aerosol loading. Although both model studies reproduced the observed enhanced trend of NO_2 relative to the growth of N_2O at the surface, the difference in their conclusions about the components contributing to the trend and their magnitudes underscores the uncertainty in the current understanding. *Zander et al.* [1998] reported an analysis of the total reactive nitrogen (NO_y) from daytime high spectral resolution infrared ground-based solar absorption measurements of NO, NO_2, HNO_3, and $ClONO_2$ recorded from the Jungfraujoch station in the Swiss Alps (46.5°N latitude, 7.98°E, 3.58 km altitude). Total columns from measurements of the three species from 1985 to 1995 observations showed excellent agreement between their measured increase rate (0.30 ± 0.06%) yr^{-1} and the rate of N_2O increase of (0.31 ± 0.05)% yr^{-1} measured above the station over the same time period.

[6] Stratospheric total reactive nitrogen has been measured by a variety of techniques including spaceborne [e.g., *Russell et al.*, 1988; *Rinsland et al.*, 1996], balloon-borne [e.g., *Sen et al.*, 1998; *Osterman et al.*, 1999], and ground-based infrared solar absorption spectroscopy [*Demoulin et al.*, 1998, 2001] and in situ lower stratospheric aircraft sampling [e.g., *Fahey et al.*, 1993], though measured changes in NO_y partitioning and trends as a function of aerosol loading are rare. The significant NO_2 total column trend is important in view of the direct effect of NO_x ($NO+NO_2$) on the catalytic destruction of stratospheric O_3 [*Fish et al.*, 2000]. Analyses of NO_y changes are complicated by diurnal variations, which are significant for NO [e.g., *Rinsland et al.*, 1984], NO_2 [e.g., *Flaud et al.*, 1983, 1988], and N_2O_5 [*Toon et al.*, 1986], all abundant NO_y components. The N_2O_5 molecule cannot be quantified from ground-based infrared measurements due to interfering absorptions.

[7] The purpose of this study is to investigate post-Pinatubo eruption changes in stratospheric NO_y partitioning based on a 10-year time series of ground-based solar infrared absorption spectra recorded from a remote, high-altitude Northern Hemisphere midlatitude station. Daily average stratospheric columns of HNO_3, NO, and NO_2 are reported taking into account the vertical sensitivity of the measurements based on averaging kernels. These results are compared with two-dimensional chemistry-transport model calculations based on version 6.1 Stratospheric Aerosol and Gas Experiment (SAGE) II monthly average aerosol surface area densities through 1999 [*Yue*, 1999] with all boundary conditions specified by the "ab baseline" trend scenario for *World Meteorological Organization* (*WMO*) [2003], including the trends of N_2O, CH_4, chlorofluorocarbons, chlorine, and bromine species as a function of time. The SAGE II time series has been extended through the end of the analysis period by repeating the 1999 values. To distinguish the effects of changes in aerosol loading from those due to the trends in the abundances of molecular species, calculations were also performed with the same model and atmospheric trends scenario, but with 1999 aerosol loading adopted for the entire time span.

2. Ground-Based Observations

[8] The infrared solar spectra were recorded with a custom-made folded Michelson interferometer [*Brault*, 1978] located on a mountaintop in the Sonora desert, a semiarid region of southeastern Arizona (31.9°N latitude, 111.6°W longitude, 2.09 km altitude). The instrument is

housed in the McMath solar telescope complex and is operated by the U.S. National Solar Observatory (NSO). Most observations were obtained at a spectral resolution of 0.01–0.02 cm^{-1} (corresponding to maximum optical path differences of 50 to 94 cm) with a weak apodizing function, either a KCl or CaF_2 beam splitter, an interference filter, and a pair of liquid-nitrogen-cooled InSb or helium-cooled As-doped Si detectors. Long-term ground-based monitoring of the HNO_3, NO, and NO_2 burdens by infrared solar absorption spectroscopy is among the high priority tasks of the Network for the Detection of Stratospheric Change (NDSC) [*Kurylo*, 1991; *Kurylo and Zander*, 2000]. Kitt Peak is an official NDSC complementary station.

3. Analysis Method

[9] The spectroscopic observations have been analyzed with SFIT2, an algorithm codeveloped at NASA Langley and the National Institute for Water and Atmospheric Research for the retrieval of vertical profiles or columns from infrared ground-based solar absorption spectra recorded with Fourier transform spectrometers (FTSs). For recent examples of SFIT2 results and references to earlier work, see *Jones et al.* [2001] and *Rinsland et al.* [2000, 2001a, 2001b, 2003]. Version 3.81 was used in the present analysis.

[10] Retrievals are performed by simultaneously fitting one or more spectral intervals ("microwindows") in one or more solar spectra over a predefined range of solar zenith angles. Profiles of one or more molecules may be retrieved simultaneously. Additionally, the a priori mixing ratio profiles of interfering molecules can be scaled over the entire altitude span by a single factor to improve the spectral fits. A Voigt shape [*Drayson*, 1976] is assumed for all lines.

[11] Inversions are based on a semiempirical application of the optimal estimation formalism of *Rodgers* [1976]. The rationale for adopting this approach has been described by *Pougatchev et al.* [1995, section 2.3]. The SFIT2 program includes a crude solar model with parameters that can simulate and fit the absorption by solar CO [*Rinsland et al.*, 1984] or solar OH lines [*Rinsland et al.*, 2003].

[12] Line-by-line calculations used a 29-layer atmospheric model with 2 km thick layers in the lower atmosphere extending from the surface to 100 km. Density-weighted pressures, temperatures, and air masses in each layer were calculated with an improved version [*Meier et al.*, 2003] of a refractive ray-tracing program [*Gallery et al.*, 1983]. Temperature profiles for each observation day were obtained from the U.S. National Centers for Environmental Prediction (NCEP). In the present analysis we report vertical profiles calculated for the 14–60 km altitude region, where 14 km corresponds to the average altitude of the tropopause above the station based on NCEP statistics (S. Zhou, and A. Miller, NCEP, private communication, 2002).

4. A Priori Profiles, Spectroscopic Parameters, and Microwindows

[13] Spectroscopic parameters and microwindows were selected based on three considerations: (1) the availability of target gas spectral features with minimal interferences from other atmospheric and solar spectral features, (2) low sensitivity of the target absorption to errors in the temperature profile, and (3) the quality of the spectroscopic parameters. Table 1 reports the selected spectral intervals for the three molecules. Selection of microwindows was guided primarily by the ground-based solar atlas of *Meier et al.* [1997], which provides molecule-by-molecule simulations and typical high resolution atmospheric spectra for the middle infrared. Minor or weakly absorbing molecules were included in the forward model calculations but not retrieved. Measurements of NO and NO_2 were restricted to solar astronomical zenith angles less than 70° to reduce the impact of diurnal changes [e.g., *Camy-Peyret et al.*, 1983; *Rinsland et al.*, 1984; *Flaud et al.*, 1988], but with sufficient observations to define seasonal variations and the long-term trend. We next describe the selection of the spectral intervals, spectroscopic parameters, the a priori profiles, and the covariance matrices for the target molecules.

4.1. Nitric Acid (HNO_3)

[14] Nitric acid is the most abundant stratospheric NO_y component below ~30 km altitude where its photochemical lifetime is on the order of days [*Brasseur and Solomon*, 1984, Figure 5.38; *Austin et al.*, 1986]. The strong ν_5 band HNO_3 Q branch at 878 cm^{-1} appears in 1950–1951 solar spectra recorded from the Jungfraujoch station (46.5°N latitude, 8.0°E longitude, 3.58 km altitude) at 0.12–0.44 cm^{-1} resolution [*Rinsland et al.*, 1991, Figures 1 and 5].

[15] The 868.5–870.0 cm^{-1} interval adopted for retrieval of HNO_3 is nearly the same as the interval selected by *Connor et al.* [1998] for analysis of solar absorption observations from Arrival Heights, Antarctica, and by *Rinsland et al.* [2000] for an analysis of lower stratospheric volume mixing ratio correlations. The vertical profile of HNO_3 was retrieved. Additionally, as a weak but detectable absorber in the interval, OCS was fitted by solving for a single factor to multiplicatively scale its a priori volume mixing ratio profile.

[16] As first noted by *Blatherwick et al.* [1991], high spectral resolution ground-based solar spectra show significant sensitivity to the lower stratospheric HNO_3 profile in this region where a series of near equally spaced P branch manifolds of the ν_5 band account for most of the absorption. This sensitivity occurs even though the individual HNO_3 lines are only partially resolved. *Hase* [2000] also concluded from his analysis of high resolution ground-based solar spectra that this spectral region is sensitive to the HNO_3 stratospheric vertical profile distribution.

[17] The HNO_3 line parameters from the 1996 HITRAN compilation [*Rothman et al.*, 1998] were updated with the recommendations of *Goldman et al.* [1998a]. Spectral parameters were taken mostly from HITRAN 2001 (available from http://www.hitran.com). Improvements in HNO_3 spectroscopy in this spectral region have been reported recently [*Toth et al.*, 2001], but the parameters have not yet been released.

[18] The HNO_3 a priori profile is based primarily on version 3 Atmospheric Trace Molecule Spectroscopy (ATMOS) recorded during the November 1994 ATLAS 3 mission [*Irion et al.*, 2002]. A mean stratospheric profile from measurements within 10° latitude of Kitt Peak was smoothly connected to a reference profile at higher altitudes and a tropospheric profile that decreased to a volume

Table 1. Microwindows, Interferences, and Range of Zenith Angles for Retrieval of HNO_3, NO, NO_2 Stratospheric Columns From the Kitt Peak Post-Pinatubo Eruption Solar Spectra[a]

Target Molecule	Microwindow, cm^{-1}	Fitted Interferences	Minor Interferences	Maximum Solar Astronomical Zenith Angle, deg
HNO_3	868.50–870.00	OCS, H_2O, O_3	CO_2, NH_3	85
NO	1899.80–1900.20	O_3, H_2O, N_2O, CO_2 solar CO	COF_2	70
NO_2	2914.60–2914.70	H_2O, CH_4 O_3		70

[a]All interfering molecules were fitted in the retrievals by multiplicative scaling of the a priori profile by a single factor.

mixing ratio (VMR) of 3.8×10^{-11} in the bottom layer (2.09–3.0 km) as described previously [*Rinsland et al.*, 2000, section 4]. The covariance matrix was assumed diagonal with relative uncertainties set equal to 0.2 times the a priori profile assumed for all 29 forward model layers. The signal-to-noise ratio was set at 500, consistent with typical measurements.

4.2. Nitric Oxide (NO)

[19] The most favorable spectral region in the infrared for measuring NO occurs near 5 μm, where the fundamental vibration-rotation band is observable via solar absorption spectroscopy from high-altitude ground-based stations [e.g., *Rinsland et al.*, 1984]. Although three vibration-rotation transitions (lambda doublets which are resolved at resolutions above 0.01 cm^{-1}) are observable from high-altitude sites such as Kitt Peak under dry conditions, only the best of the three containing the P(8.5) transition at 1900.08 cm^{-1} was fitted in our analysis. The selected interval extending from 1899.80 to 1900.20 cm^{-1} was fitted for the profile of NO in solar spectra recorded at solar zenith angles less than 70° to limit changes due to diurnal stratospheric chemistry, as previously mentioned. Identifications of atmospheric features in the region have been reported previously [*Rinsland et al.*, 1984, Table 2 and Figure 1]. We assumed a signal-to-noise ratio of 500, consistent with typical measurements, a diagonal covariance matrix, and a reference daytime NO a priori profile increasing from 0.3 parts per billion (10^{-9}) by volume (ppbv) below 12 km to 0.35 ppbv at 23 km, then rising rapidly with altitude to 10 ppbv at 42 km with higher mixing ratios above. A diagonal covariance matrix was assumed. Spectroscopic parameters for NO were adopted from the 1996 HITRAN compilation and were described by *Goldman et al.* [1998b].

4.3. Nitrogen Dioxide (NO_2)

[20] The best region for measurement of NO_2 from ground-based infrared solar spectra occurs near 3 μm where the $\nu_1 + \nu_3$ band produces the strongest absorption [*Camy-Peyret et al.*, 1983; *Flaud et al.*, 1983, 1988]. A narrow microwindow from 2914.60 to 2914.70 cm^{-1} was selected for the analysis. A signal-to-noise ratio of 500, a relative uncertainty of 0.5 in each layer, and a diagonal covariance matrix were assumed. The a priori NO_2 profile was adopted from reprocessed Limb Infrared Monitor of the Stratosphere (LIMS) measurements recorded at 32°N latitude during March 1979 near noon local time (M. Natarajan, private communication, 2002). The volume mixing ratio increases from 0.3 ppbv below 12 km to 1.0 ppbv at 21 km, reaching a maximum of 5.59 ppbv at 33 km, declining above. The spectral interval also contains weak absorptions by CH_4 and O_3. Each interfering molecule was fitted scaling its a priori profile by a single multiplicative factor. Spectroscopic parameters for NO_2 were taken from HITRAN 2001, as reported on the HITRAN website. They are based on the work of *Mandin et al.* [1997] and include updates to the positions, intensities, and air-broadening coefficients. Spectroscopic parameters for OCS were added from the HITRAN 2001 database, as the molecule is a weak absorber in the microwindow selected for NO_2 retrievals.

5. Measurement Results

[21] Figure 1 presents 14–60 km column averaging kernels for the three target molecules plotted versus altitude. The altitude range corresponds approximately to the stratosphere above the station. The averaging kernels show how the true profile and a priori one contribute to the retrieved column for the layer [*Rodgers*, 1976, 1990; *Pougatchev et al.*, 1995, 1996]. The averaging kernels for each of the three molecules are broad and increase with height in the lower stratosphere. Only HNO_3 reaches a distinct maximum, located at 25 km. The 14–60 km column kernels of NO and NO_2 have broad maxima around 34 km.

[22] Figure 2 presents sample fits for NO, NO_2, and HNO_3 after excluding noisy spectra and measurements of weak absorption based on objective criteria [*Rinsland et al.*, 1998, Figure 9]. Each spectrum has been normalized to the highest value in the fitted interval. Arrows mark the location of the target NO and NO_2 absorption lines. The resolution

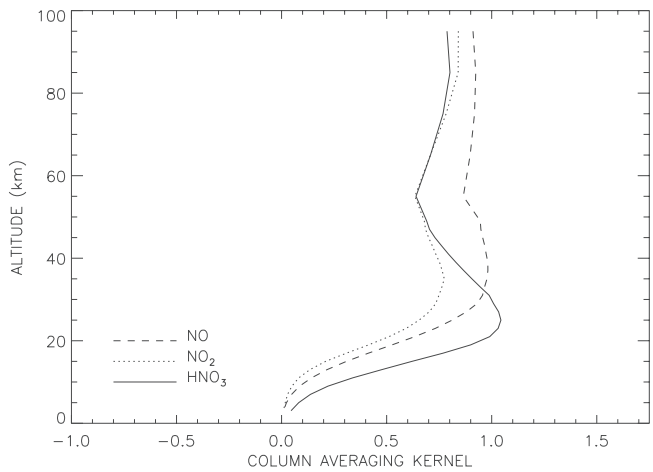

Figure 1. Column averaging kernels for merged layers from 14–60 km altitude plotted versus height for NO, NO_2, and HNO_3.

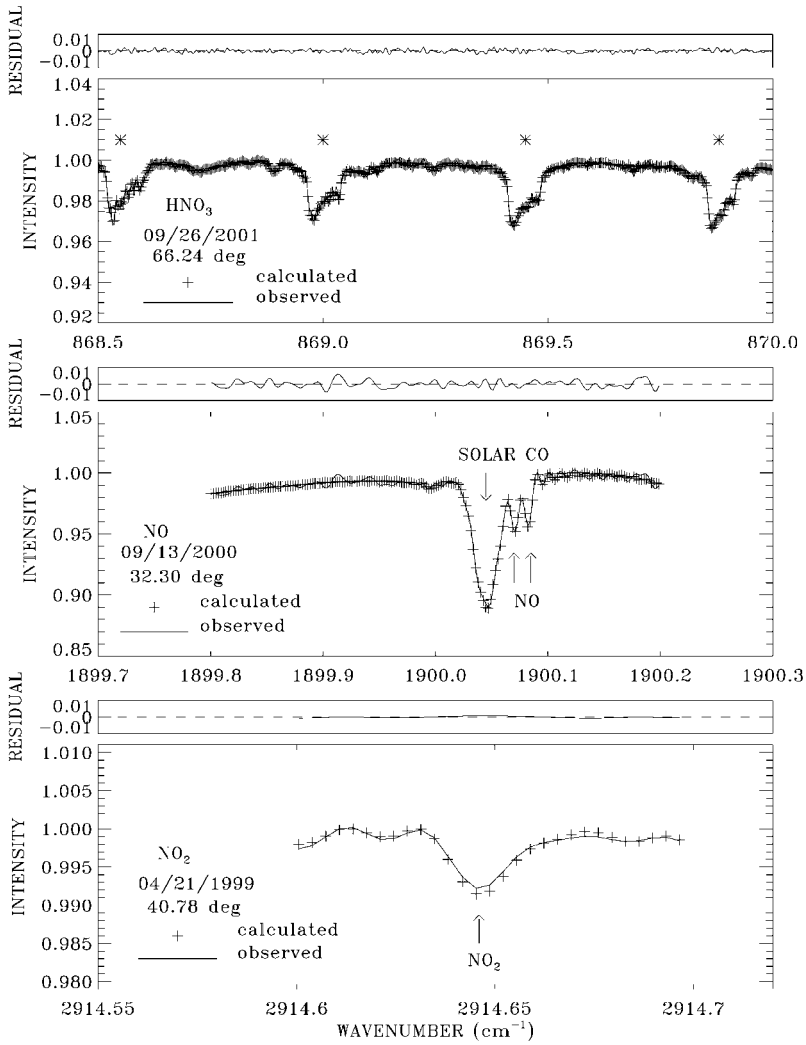

Figure 2. Sample normalized measured spectrum and fit for (top) HNO_3, (middle) NO, and (bottom) NO_2. Astronomical zenith angles and dates of observation are indicated. The HNO_3 region spans four unresolved P branch ν_5 band manifolds, which are marked by asterisks. The single NO interval shows a solar CO line adjacent to the resolved NO doublet. The NO_2 spectrum contains a single atmospheric feature marked with an arrow. The panel above each measured spectrum shows the residuals (measured minus fitted values).

of the Kitt Peak spectra is sufficient throughout most the time series to resolve the two lambda-doublet NO components, as illustrated. Residuals (measured minus calculated) are shown above. The first post-Mount Pinatubo eruption measurements meeting the quality selection criteria were recorded in March 1992, July 1991, and November 1991 for HNO_3, NO, and NO_2, respectively. The number of days with measurements was 151, 103, and 124, respectively. All reported results are daily averages.

6. Measurement Error Budget

[23] Table 2 presents evaluation of the sources of random and systematic error and provides estimates of the uncertainties in the daily average stratospheric columns of each molecule. Error budget calculations were performed similar to those in previous studies [e.g., *Rinsland et al.*, 1998]. Errors due to diurnal changes in the stratospheric columns were regarded as a random source of error as the measurements were recorded different times of the day with no fixed sampling pattern. Estimates of the error in assuming an average from observations at less than a 70° zenith angle were based on previous studies of the Kitt Peak spectra of NO [*Rinsland et al.*, 1984] and NO_2 [*Flaud et al.*, 1983, 1988] daytime diurnal variations. The finite signal-to-noise ratio of the NO_2 measurements was also a significant source of random error as the target spectral feature was weak in the measured spectra for the limited range of zenith angles included. The dominant sources of systematic error were the uncertainty in the spectroscopic parameters and the relative contribution of the a priori to the retrieval, the latter was especially important in NO_2.

7. Model Calculations

[24] Model calculations were performed with the Atmospheric and Environmental Research, Inc. (AER) two-dimensional chemical-transport model [*Shia et al.*, 1998;

Table 2. Estimated HNO_3, NO, and NO_2 14–60 km 1-sigma Uncertainties for Daily Averages[a]

Error Source	Uncertainty, %		
	HNO_3	NO	NO_2
Random Errors			
Temperature profile	<1	<1	<1
Finite signal to noise	1	1	5
Interfering atmospheric lines	1	2	1
Zenith angle uncertainty	1	1	1
Zero level offsets	<1	<1	<1
Diurnal changes	0	10	10
RSS total random error	1	11	11
Systematic Errors			
Spectroscopic parameters	5	5	5
A priori profile relative contribution	−4	5	36
Forward model approximations	2	2	2
Instrument line shape function	<1	<1	<1
Zero transmittance offsets	<1	<1	<1
RSS total systematic error	7	7	36

[a]RSS, root-sum-square deviation computed from the estimates of errors for the individual error sources.

Weisenstein et al., 1997, 1998]. The model domain extends from the ground to 60 km with a vertical resolution of approximately 1.2 km and from pole to pole with horizontal resolution of 5° for these calculations. Model temperatures and transport/circulation are prescribed according to climatology and do not respond to changes in aerosols or chemical species. Monthly zonal mean temperatures from the National Centers for Environmental Prediction reanalysis project were used [*Kalnay et al.*, 1996], along with statistics for deviations from the zonal monthly mean. Years prior to 1996 used temperature fields for the year modeled, while subsequent years used a 1979–1995 climatology. Residual circulation and eddy diffusion coefficients used were from the NASA Goddard Space Flight Center 2-D model [*Jackman et al.*, 1996; *Fleming et al.*, 1999] and were calculated for observed climatological values of temperature, H_2O, zonal wind, and ozone.

[25] The model includes full O_x, HO_x, CHO_x, NO_x, ClO_x, and BrO_x photochemistry. The family approach is used to constrain the sum of reactive nitrogen species to equal the total transported NO_y. Boundary conditions for the long-lived species (e.g., CH_4, N_2O, and chlorinated source gases) follow historical trends [*Chipperfield and Randel*, 2003], adopted as the Ab baseline trend scenario for *WMO* [2003]. The diurnal concentrations of radical species are calculated 17 times per day with time points that depend on the length of the day. Nighttime is modeled with 5 equally spaced points. There also are points exactly at sunrise, sunset, and at 90° zenith angles. Daytime changes are modeled with 10 equally spaced points in time between the 90° zenith angle points. Recent recommended changes in reaction rates [*Brown et al.*, 1999a, 1999b] that improve the agreement between observed and modeled NO_x/NO_y were incorporated into the model based on JPL 2000 [*Sander et al.*, 2000]. Although convection and lightning sources are included in the model, the lower stratospheric calculations may be less accurate as the model omits anthropogenic surface sources of NO_y emissions and there are strong gradients near the tropopause that are difficult to accurately characterize. As illustrated by Figure 1, the measurements have low sensitivity in the tropopause region, so the averaging kernel will place less weight here in the column integration.

[26] Sulfate aerosol surface area density [*Yue*, 1999] from version 6.1 SAGE II data was used through the end of 1999. Missing data points from early in the post-Pinatubo period were filled with surface area density calculated by the AER 2-D sulfate aerosol model [*Weisenstein et al.*, 1997] and later in the period from *Chipperfield and Randel* [2003] values. The time series was extended to 2002 by repeating the 1999 values for subsequent years.

8. Model-Measurement Comparison

[27] Figures 3a–3c display the HNO_3, NO, and NO_2 Kitt Peak post-Pinatubo eruption measurements extending to November 2002, chemical model calculations for 32.5°N latitude, the closest AER prediction to Kitt Peak, and a statistical fit to the measured time series. The assumed aerosol surface area density time series for the same latitude and an altitude of 25 km is displayed in Figure 3d. The measurements are daily averages displayed with open triangles. The number of Kitt Peak measurements per day ranged from 1 to 20 for HNO_3, 1 to 13 for NO, and 1 to 13 for NO_2, with more frequent measurements during the last several years as a consequence of an increased commitment to the NDSC. The total number of measurements in the database is 151 for HNO_3, 103 for NO, and 129 for NO_2. As can be seen from Figure 3, the database of measurements shortly after the Mount Pinatubo eruption is sparse with not all species measured on some days. The pluses show the model results combined with the averaging kernel [*Connor et al.*, 1995, equation (12)], which explicitly shows how high vertical resolution measurements or model results are smoothed by the measurement and retrieval process. Fits to the time series with and without a modeled seasonal cycle are shown with solid and dashed lines, respectively.

[28] The time series of measured 14–60 km columns were fitted with the expression

$$C_A = a_0 + a_1(t - t_0) + a_2(t - t_0)^2 + a_3 \cos[2\pi(t - t_0 - \varphi)], \quad (2)$$

where C_A is the daily average 14–60 km column at time t, t_0 is the time of the first measurement, a_0 is the initial ($t = t_0$) annual mean 14–60 km column of the time series, a_1 and a_2 are coefficients for modeling the long-term trend, a_3 is the amplitude of the seasonal cycle, and φ is the phase corresponding to the seasonal maximum.

[29] All three molecules show long-term trends in the 14–60 km column with the largest change being the decline in the stratospheric column of HNO_3. Normalized to the mean 14–60 km column and after fitting the full time series with equation (2) (including the seasonal variation), the measurements show a 20% decline in the stratospheric HNO_3 column from the time of the first post-Pinatubo observation in March 1992 until the beginning of 1996, reaching a broad minimum about 25% below the peak after the return to background aerosol loading. Normalized to the mean, the best fit long-term HNO_3 trend (1992–2002) and its 1-sigma uncertainty equal $(-6.14 \pm 1.15)\%\ yr^{-1}$ for a_1 and $(+0.39 \pm 0.10)\%\ yr^{-2}$ for a_2. Although a slight rise is predicted at the end of the time series, it is within the measurement error; extrapolation of the trend with this

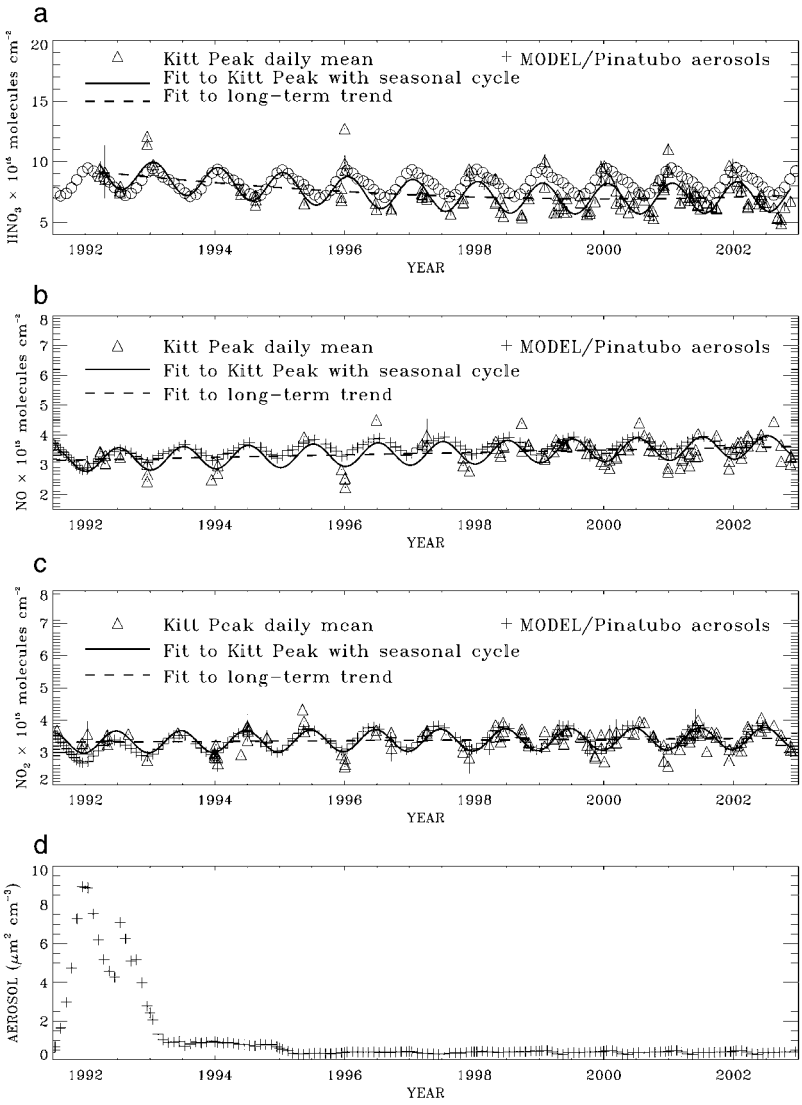

Figure 3. Kitt Peak measured and model-calculated 14–60 km columns at 32.5°N latitude for (a) HNO_3, (b) NO, and (c) NO_2 and (d) sulfate aerosol surface area density at 25 km time series plotted versus time for the Mount Pinatubo and post-Pinatubo eruption period. Measured daily average columns are shown with open triangles. Measurements for NO and NO_2 are restricted to astronomical zenith angles of 70° or less. Model profiles have been combined with the column averaging kernels. Solid curves in Figures 3a–3c show fits to the time series with equation (2) (a_2 set to zero for NO and NO_2). The best fit to the measured long-term trend is shown with a dashed line. Model calculations are displayed with plus symbols.

polynomial expression and best fit coefficients is inappropriate. For NO and NO_2, a_2 values are constrained to zero, as they could not be determined with statistical significance. The long-term trends and corresponding one sigma uncertainty for fits to the full time series based on the daytime daily averages equal (+1.56 ± 0.45)% yr^{-1} for NO, and (+0.49 ± 0.29)% yr^{-1} for NO_2. Fits to the daily averages yield a winter maximum for HNO_3 and summer maximum for both NO and NO_2. As the amplitudes are only ~10% relative to the mean, determination of the times of the seasonal maxima are subject to considerable uncertainty due to the limited sampling and day-to-day fluctuations resulting from transport of lower and higher latitude air to above the station.

[30] Figure 4 illustrates the impact of the Mount Pinatubo eruption on the model-calculated HNO_3, NO, and NO_2 14–60 km time series. Plotted is the ratio of the model-calculated columns with Pinatubo aerosols divided by a corresponding calculation without Pinatubo aerosols but with seasonally varying background aerosols used for all years. The assumed variation of background aerosol loading versus time is illustrated in the bottom panel; it assumes the same seasonal variation as illustrated in Figure 3d for post-1999. For consistency with the measured data and the model calculations in Figure 3, the model profiles used to generate Figure 4 have been combined with the Kitt Peak averaging kernels. Boundary conditions from the *WMO* [2003] Ab baseline trend scenario have been retained.

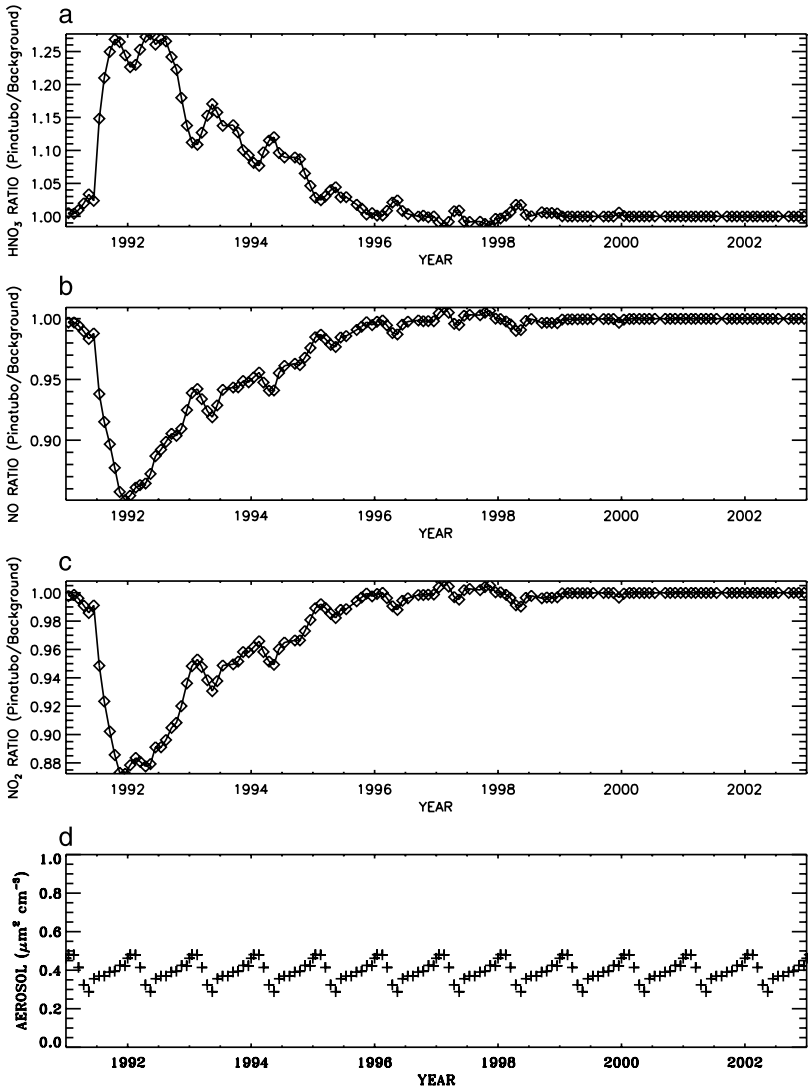

Figure 4. AER 2-D model-calculated time evolution of the ratio of average-kernel-weighted 14–60 km columns of (a) HNO_3, (b) NO, and (c) NO_2 versus time for the Mount Pinatubo and post-Mount Pinatubo eruption time period to (d) model values for the assumed background aerosol loading at 25 km.

[31] The ratios in Figure 4 versus time allow the impact of the aerosol loading on the stratospheric columns of the three molecules to be assessed as a function of time. Ratios for HNO_3 as a function of time declined from a maximum of 1.27 near the end of 1991 and the beginning of 1992, decreasing to 1.02 at the start of 1995, and reached 1.00 at the beginning of 2002. The ratio from the model calculations near the beginning of 1992 is roughly consistent with the observed ratio of HNO_3 in early 1992 to that in early 1996 using the limited set of measurements from this time period. The ratio for NO increased from 0.85 at the start of 1992 to 0.98 at the beginning of 1995, reaching 1.00 in 2002. Corresponding values for the NO_2 14–60 km column were 0.87, 0.99, and 1.00. Unfortunately, measurements of NO and NO_2 shortly after the Mount Pinatubo eruption are too sparse and the depletions too small relative to the precision to provide a quantitative confirmation of the predicted column decreases.

[32] We conclude from Figure 4 that the impact of aerosol loading changes on the stratospheric HNO_3, NO, and NO_2 columns was limited almost entirely to the first 4 years after the eruption with larger stratospheric column changes for HNO_3 than for NO and NO_2. Total NO_y column amounts in the model are not modified significantly by the large perturbation in stratospheric aerosol loadings, only the partitioning of NO_y was changed. *Zander et al.* [1998] noted a recovery to baseline (pre-1988) NO_y levels above the Jungfraujoch station by the end of 1994.

[33] The changes in HNO_3, NO, and NO_2 seen in Figure 3 from ~1995 to 2002 are expected to be mainly due to increasing levels of stratospheric NO_y caused by increasing N_2O at the surface. However, as already mentioned, changes in H_2O, temperature, aerosol loading, halon loading, ozone, and shifts in NO_y partitioning are predicted by models to also modify stratospheric NO_y and partitioning into its components [*Fish et al.*, 2000; *McLinden et al.*, 2001]. Additionally, lightning-generated NO or changes in circulation could modify long-term stratospheric trends.

[34] As an attempt to understand changes during the less variable period of background aerosol loading, we restrict

our analysis to the measurements to 1995–2002 and analyzed this 7-year time span to determine linear trends as a function of time (a_2 in equation (2) set to zero). Measured trends relative to the mean for the 14–60 km altitude range are $(-0.36 \pm 0.63)\%$ yr^{-1} for HNO_3, $(+1.28 \pm 0.76)\%$ yr^{-1} for NO, and $(+1.03 \pm 0.55)\%$ yr^{-1} for NO_2, 1 sigma. Considering the mean, the 1-sigma uncertainty, and the scatter in the trends, our post-Pinatubo increase rates are broadly consistent with both the average rate of N_2O growth of $(0.31 \pm 0.05)\%$ yr^{-1} measured from 1985–1995 infrared ground-based solar spectra recorded from the Jungfraujoch [*Zander et al.*, 1998], $(0.36 \pm 0.06)\%$ yr^{-1} from 1984–1992 from global tropospheric measurements [*WMO*, 1999, Table 1–2], and the anomalous stratospheric NO_2 increase rate of 5% per decade from 1980 to 1998 slant column visible (zenith scattered) ultraviolet-visible measurements at 45°S latitude [*Liley et al.*, 2000]. Differences in the best fit trends for the three species measured above Kitt Peak underscores the difficulty in determining precise long-term trends from measurements with limited temporal sampling superimposed on seasonal and short-term variability, even for one of the longest databases of observations in the NDSC.

9. Discussion

[35] As summarized in the introduction, numerous studies reported elevated concentrations or columns of HNO_3 shortly after the Mount Pinatubo eruption with decreased concentrations of NO_x and N_2O_5 due to the effects of reaction (1) on NO_y repartitioning at the high sulfate aerosol loading at that time. Our study has tracked the changes in stratospheric HNO_3, NO, and NO_2 columns as lower-stratospheric sulfate aerosol loading declined by a factor of ~20 over a 10-year period. Normalized to the mean stratospheric column and including modeling of the seasonal changes, a best fit to HNO_3 shows a decline of 20% from 1992 to the beginning of 1996, followed by a further decline reaching a broad minimum 25% below the peak at the end of the observation period. Smaller relative changes in the 14–60 km columns are observed for NO and NO_2, consistent with the model predictions displayed in Figure 4.

[36] To our knowledge, our study is the first to document the reduced impact of reaction (1) on NO_y partitioning as aerosol loading from the Mount Pinatubo eruption has declined to background levels. *Van Allen et al.* [2002, Figure 2] reported HNO_3 total column measurements from June 1991 to June 2000 from the NDSC station on Mauna Loa, Hawaii (19.5°N, 155.6°W, 3.40 km altitude). They reported a 30% HNO_3 total column decrease from 1991 to 1996 followed by no apparent trend during the remainder of their time series, which ended in June 2000. No evidence or discussion of seasonal changes was reported. Our measured HNO_3 long-term post-Pinatubo trend is similar to their results though we improved the precision in the trend determination by modeling the observed seasonal variation. As displayed in Figure 3, the AER model predicts stratospheric columns and seasonal variations for all three molecules in excellent agreement with our observations. The 1985–1995 Jungfraujoch time series [*Zander et al.*, 1988; *DeMazière et al*, 1998] documented effects of the Mount Pinatubo enhanced aerosol loading on NO_y partitioning shortly after the eruption with maximum NO_2 total column reductions of 40–45% in December 1991 to January 1992, less than the model predicted NO_2 loss in Figure 4, but consistent with the slant column depletion reported by *Liley et al.* [2000].

10. Summary and Conclusions

[37] A 10-year time series of ground-based infrared solar spectra recorded following the massive June 1991 Mount Pinatubo volcanic eruption has been analyzed to derive trends in the stratospheric columns of HNO_3, NO, and NO_2 during this period of declining stratospheric sulfate aerosol loading. The largest changes are observed for HNO_3 with an overall decline of 20% from 9.16×10^{15} molecules cm^{-2} at the time of first observation in March 1992 to 7.40×10^{15} molecules cm^{-2} at the start of 1996 reaching a broad minimum of 6.95×10^{15} molecules cm^{-2}, 25% below the first post-Pinatubo observation by the end of the time series. Smaller long-term changes are observed for NO and NO_2 based on daytime measurements restricted to a solar zenith angle of 70° or less. The long-term trends of all three molecules are superimposed on seasonal cycles with peak amplitudes of ~10% relative to the mean and day-to-day variations.

[38] The measurements and model time series have been compared with 2-D model calculations utilizing version 6.1 SAGE II aerosol surface area density profiles through 1999 and extended to the end of the measurement time series by repeating the 1999 values, retaining the seasonal cycle. Temperatures from NCEP were assumed. The measured stratospheric column trends are consistent with the two-dimensional model calculations after taking into account the vertical stratospheric column sampling sensitivity based on the averaging kernels with agreement to ~6% for HNO_3, ~2% for NO, and ~8% for NO_2, the most difficult species to measure when limiting the observations to a zenith angle of 70° due to its weak absorption. Overall, the consistency between the measured and model-calculated time series confirms the declining impact of the key heterogeneous reaction that converts reactive nitrogen to its less active reservoir form and lessens its impact on stratospheric ozone. Trends of the NO, NO_2, and HNO_3 stratospheric columns for the 1995–2002 period of lower aerosol loading are broadly consistent with the growth rate of surface N_2O during that time span and the higher average growth rate of 5% per decade reported from 1980–1998 slant path visible stratospheric NO_2 measurements [*Liley et al.* [2000]. Additional, more frequent measurements in conjunction with model calculations are needed to improve the precision in the determinations of the stratospheric column long-term trends of HNO_3, NO, and NO_2 and understand causes in view of the discrepancy between the surface N_2O increase rate and the higher reported stratospheric NO_2 rate of increase.

[39] **Acknowledgments.** Research at the NASA Langley Research Center was supported by NASA's Upper Atmosphere Research Program and the Atmospheric Chemistry, Modeling, and Analysis (ACMAP) program Research at AER was supported by ACMAP (NASW-00138) and the SAGE II program (NAS1-20666). The National Solar Observatory (NSO) is operated by the Association of Universities for Research in Astronomy, Inc. (AURA) under cooperative agreement with the National Science Foundation (NSF) with the present measurements also supported by NASA.

Work at the University of Liège was primarily supported by the Federal Office for Scientific, Technical, and Cultural Affairs (OSTC) and by the European Commission Directorate General (EC-DG), both in Brussels, Belgium. The authors thank Aaron Goldman of the University of Denver for assistance in obtaining the NCEP profiles and pointing out the missing OCS lines in the NO_2 spectral region. We also thank Charles Jackman and Eric Fleming of NASA Goddard Spaceflight Center for use of their 2-D model transport parameters and the referees for suggestions and corrections to the text and references.

References

Austin, J., R. R. Garcia, J. M. Russell III, S. Solomon, and A. F. Tuck, On the atmospheric photochemistry of nitric acid, *J. Geophys. Res.*, *91*, 5477–5485, 1986.

Blatherwick, R. D., F. J. Murcray, D. G. Murcray, and M. H. Locker, Determination of the altitude of the nitric acid layer from very high-resolution ground-based solar spectra, *Proc. SPIE Int. Soc. Opt. Eng.*, *1491*, 203–210, 1991.

Brasseur, G., and C. Granier, Mount Pinatubo aerosols, chlorofluorocarbons, and ozone depletion, *Science*, *257*, 1239–1242, 1992.

Brasseur, G., and S. Solomon, *Aeronomy of the Middle Atmosphere*, 441 pp., D. Reidel, Norwell, Mass., 1984.

Brault, J. W., Solar Fourier transform spectroscopy, in *Proceedings of the JOSO Workshop, Future Solar Optical Observations, Needs and Constraints, Firenze, Italy*, edited by G. Godoli, G. Noci, and A. Reghin, pp. 32–52, Baccini and Chiappi, Florence, Italy, 1978.

Brown, S. S., R. K. Talukdar, and A. R. Ravishankara, Reconsideration of the rate constant for the reaction of hydroxyl radicals with nitric acid, *J. Phys. Chem. A*, *103*, 3031–3037, 1999a.

Brown, S. S., R. K. Talukdar, and A. R. Ravishankara, Rate constants for the reaction $OH + NO_2 + M \rightarrow HNO_3 + M$ under atmospheric conditions, *Chem. Phys. Lett.*, *299*, 277–284, 1999b.

Camy-Peyret, C., J.-M. Flaud, J. Laurent, and G. M. Stokes, First infrared measurement of atmospheric NO_2 from the ground, *Geophys. Res. Lett.*, *10*, 35–38, 1983.

Chipperfield, M., and W. Randel, Global ozone: Past and future, in *Scientific Assessment of Ozone Depletion 2002*, *Rep. 47*, pp. 4.1–4.91, WMO Global Ozone Res. and Monit. Proj., Geneva, 2003.

Connor, B. J., A. Parrish, J.-J. Tsou, and M. P. McCormick, Error analysis for the ground-based microwave ozone measurements during STOIC, *J. Geophys. Res.*, *100*, 9283–9291, 1995.

Connor, B. J., N. B. Jones, S. W. Wood, J. G. Keys, C. P. Rinsland, and F. J. Murcray, Retrieval of HCl and HNO_3 profiles from ground-based FTIR data using SFIT2, in *Atmospheric Ozone: Proceedings of the XVIII Quadrennial Ozone Symposium, L'Aquila, Italy, September 12–21, 1996*, edited by R. D. Bojkov and G. Visconti, pp. 485–488, Edigrafital, Teramo, Italy, 1998.

Considine, D. B., A. R. Douglass, and R. S. Stolarski, Heterogeneous conversion of N_2O_5 to HNO_3 on background stratospheric aerosols: Comparison of model results with data, *Geophys. Res. Lett.*, *19*, 397–400, 1992.

David, S. J., F. J. Murcray, A. Goldman, C. P. Rinsland, and D. G. Murcray, The effect of the Mt. Pinatubo aerosol on the HNO_3 column over Mauna Loa, Hawaii, *Geophys. Res. Lett.*, *21*, 1003–1006, 1994.

DeMazière, M., M. Van Roozendael, C. Hermans, P. C. Simon, P. Demoulin, G. Roland, and R. Zander, Quantitative evaluation of the post-Mount Pinatubo NO_2 reduction and recovery, based on 10 years of Fourier transform infrared and UV-visible spectroscopic measurements and Jungfraujoch, *J. Geophys. Res.*, *103*, 10,849–10,858, 1998.

DeMore, W. B., S. P. Sander, D. M. Golden, R. F. Hampson, M. J. Kurylo, C. J. Howard, A. R. Ravishankara, C. E. Kolb, and M. J. Molina, Chemical kinetics and photochemical data for use in stratospheric modeling, *JPL Publ. 97-4*, 1997.

Demoulin, P., E. Mahieu, R. Zander, G. Roland, L. Delbouille, C. Servais, M. De Mazière, and M. Van Roozendael, The current budget of NOy above the Jungfraujoch as derived from IR solar observations, in *Proceedings of the Fourth European Symposium "Polar Stratospheric Ozone, 1997," Schliersee, Germany, September 22–26, 1997*, *Air Pollut. Res. Rep. 66*, pp. 427–430, Eur. Comm., Brussels, 1998.

Demoulin, P., E. Mahieu, R. Zander, B. Rognerud, I. Isaksen, and M. DeMazière, The NO_y budget above the Jungfraujoch: Long-term evolution, family partition, and model comparison, paper 4-05 presented at NDSC 2001 Symposium, Session 4, Ozone-Related Chemical Species: Distributions and Trends, Network for Detection of Stratosphere Change, Arcachon, France, 24 –27 Sept. 2001.

Drayson, S. R., Rapid computation of the Voigt function, *J. Quant. Spectrosc. Radiat. Transfer*, *16*, 611–614, 1976.

Fahey, D. W., et al., In situ measurements constraining the role of sulphate aerosols in mid-latitude ozone depletion, *Nature*, *363*, 509–514, 1993.

Fish, D. J., H. K. Roscoe, and P. V. Johnston, Possible causes of stratospheric NO_2 trends observed at Lauder, New Zealand, *Geophys. Res. Lett.*, *27*, 3313–3316, 2000.

Flaud, J.-M., C. Camy-Peyret, D. Cariolle, J. Laurent, and G. M. Stokes, Daytime variation of atmospheric NO_2 from ground-based infrared measurements, *Geophys. Res. Lett.*, *10*, 1104–1107, 1983.

Flaud, J.-M., C. Camy-Peyret, J. W. Brault, C. P. Rinsland, and D. Cariolle, Nighttime and daytime diurnal variation of atmospheric NO_2 from ground-based infrared measurements, *Geophys. Res. Lett.*, *15*, 261–264, 1988.

Fleming, E. L., C. H. Jackman, R. S. Stolarski, and D. B. Considine, Simulation of stratospheric tracers using an improved empirically based two-dimensional model transport formulation, *J. Geophys. Res.*, *104*, 23,911–23,934, 1999.

Gallery, W. O., F. X. Kneizys, and S. A. Clough, Air mass computer program for atmospheric transmittance/radiance calculation: FSCATM, *Environ. Res. Pap. 828 (AFGL-TR-0065)*, 145 pp. Air Force Geophys. Lab., Bedford, Mass., 1983.

Gao, R. S., et al., A comparison of observations and model simulations of NO_x/NO_y in the lower stratosphere, *Geophys. Res. Lett.*, *26*, 1153–1156, 1999.

Godin, S., L. R. Poole, S. Bekki, T. Deshler, N. Larsen, and T. Peter, Global distribution and changes in stratospheric particles, in *Scientific Assessment of Ozone Depletion: 1998*, *Rep. 44*, pp. 3.1–3.40, WMO Global Ozone Res. and Monit. Proj., Geneva, 1999.

Goldman, A., C. P. Rinsland, A. Perrin, and J.-M. Flaud, HNO_3 line parameters: 1996 HITRAN update and new results, *J. Quant. Spectrosc. Radiat. Transfer*, *60*, 851–861, 1998a.

Goldman, A., L. R. Brown, W. G. Schoenfild, M. N. Spencer, C. Chackerian Jr., L. P. Giver, H. Dothe, C. P. Rinsland, L. H. Coudert, V. Dana, and J.-Y. Mandin, Nitric oxide line parameters: Review of 1996 HITRAN update and new results, *J. Quant. Spectrosc. Radiat. Transfer*, *60*, 825–838, 1998b.

Hanson, D. R., and A. R. Ravishankara, The reaction probabilities of ClONO_2 and N_2O_5 on 40 to 75% sulfuric acid solutions, *J. Geophys. Res.*, *96*, 17,307–17,314, 1991.

Hase, F., Retrieval of trace gas profiles from high resolution, ground-based FTIR measurements, *Wis. Ber. FZKA6512*, Forsch. Karlsruhe, Karlsruhe, Germany, 2000.

Hofmann, D. J., and S. Solomon, Ozone destruction through heterogeneous chemistry following the eruption of El Chichón, *J. Geophys. Res.*, *94*, 5029–5041, 1989.

Irion, F. W., et al., The Atmospheric Trace Molecule Spectroscopy Experiment (ATMOS) version 3 data retrievals, *Appl. Opt.*, *41*, 6968–6979, 2002.

Jackman, C. H., E. L. Fleming, S. Chandra, D. B. Considine, and J. E. Rosenfield, Past, present, and future modeled ozone trends with comparisons to observed trends, *J. Geophys. Res.*, *101*, 28,753–28,767, 1996.

Jones, N. B., C. P. Rinsland, J. B. Liley, and J. Rosen, Correlation of aerosol and carbon monoxide at 45°S: Evidence of biomass burning emissions, *Geophys. Res. Lett.*, *28*, 709–712, 2001.

Jucks, K. W., D. G. Johnson, K. V. Chance, W. A. Traub, and R. J. Salawitch, Nitric acid in the middle stratosphere as a function of altitude and aerosol loading, *J. Geophys. Res.*, *104*, 26,715–26,723, 1999.

Kalnay, E., et al., The NCEP/NCAR 40-year reanalysis project, *Bull. Am. Meteorol. Soc.*, *77*, 437–471, 1996.

Koike, M., N. B. Jones, W. A. Matthews, P. V. Johnston, R. L. McKenzie, D. Kinnison, and J. Rodriguez, Impact of Pinatubo aerosols on the partitioning between NO_2 and HNO_3, *Geophys. Res. Lett.*, *21*, 597–600, 1994.

Kurylo, M. J., Network for the detection of stratospheric change, *Proc. Soc. Photo. Opt. Instrum. Eng.*, *1491*, 169–174, 1991.

Kurylo, M. J., and R. J. Zander, The NDSC—Its status after ten years of operation, paper presented at XIX Quadrennial Ozone Symposium, Hokkaido Univ., Sapporo, Japan, 3 –8 July 2000. (Available at http://www.ndsc.ws)

Liley, J. B., P. V. Johnson, R. L. McKenzie, A. J. Thomas, and I. S. Boyd, Stratospheric NO_2 variations from a long time series at Lauder, New Zealand, *J. Geophys. Res.*, *105*, 11,633–11,640, 2000.

Mandin, J.-Y., et al., The $\{\nu_1 + 2\nu_2, \nu_1 + \nu_3\}$ bands of $^{14}N^{16}O_2$: Line positions and intensities; line intensities in the $\nu_1 + \nu_2 + \nu_3 - \nu_2$ hot band, *J. Mol Spectrosc.*, *181*, 379–388, 1997.

McLinden, C. A., S. C. Olsen, M. J. Prather, and J. B. Liley, Understanding trends in stratospheric NO_y and NO_2, *J. Geophys. Res.*, *106*, 27,787–27,793, 2001.

Meier, A., G. C. Toon, C. P. Rinsland, and A. Goldman, Spectroscopic atlas of atmospheric microwindows in the middle infra-red, *Reprint 123*, 263 pp., Swed. Inst. of Space Phys., Kiruna, Sweden, 1997.

Meier, A., A. Goldman, P. S. Manning, T. M. Stephen, C. P. Rinsland, N. B. Jones, and S. W. Wood, Improvements to air mass calculations from

ground-based infrared measurements, *J. Quant. Spectrosc. Radiat. Transfer*, in press, 2003.

Osterman, G. B., B. Sen, G. C. Toon, R. L. Salawitch, J. J. Margitan, J.-F. Blavier, D. W. Fahey, and R. S. Gao, Partitioning of NO_y species in the summer Arctic stratosphere, *Geophys. Res. Lett.*, *26*, 1157–1160, 1999.

Poole, L. R., R. L. Jones, M. J. Kurylo, and A. Wahner, *Heterogeneous Processes: Laboratory, Field, and Modeling Studies*, in Scientific Assessment of Ozone Depletion: 1991, *Rep. 25*, pp. 3.1–3.17, WMO Global Ozone Res. and Monit. Proj., Geneva, 1992.

Pougatchev, N. S., B. J. Connor, and C. P. Rinsland, Infrared measurements of the ozone vertical distribution above Kitt Peak, *J. Geophys. Res.*, *100*, 16,689–16,697, 1995.

Pougatchev, N. S., B. J. Connor, N. B. Jones, and C. P. Rinsland, Validation of ozone profile retrievals from ground-based solar spectra, *Geophys. Res. Lett.*, *23*, 1637–1640, 1996.

Rinsland, C. P., R. E. Boughner, J. C. Larsen, G. M. Stokes, and J. W. Brault, Diurnal variations of atmospheric nitric oxide: Ground-based infrared spectroscopic measurements and their interpretation with time-dependent photochemical model calculations, *J. Geophys. Res.*, *89*, 9613–9622, 1984.

Rinsland, C. P., R. Zander, and P. Demoulin, Ground-based infrared measurements of HNO_3 total column abundances: Long-term trend and variability, *J. Geophys. Res.*, *96*, 9379–9389, 1991.

Rinsland, C. P., M. R. Gunson, M. C. Abrams, L. L. Lowes, R. Zander, E. Mahieu, A. Goldman, M. K. W. Ko, J. M. Rodriguez, and N. D. Sze, Heterogeneous conversion of N_2O_5 to HNO_3 in the post-Mount Pinatubo eruption stratosphere, *J. Geophys. Res.*, *99*, 8213–8219, 1994.

Rinsland, C. P., et al., ATMOS measurements of $H_2O + 2CH_4$ and total reactive nitrogen in the November 199 Antarctic stratosphere: Dehydration and denitrification in the vortex, *Geophys. Res. Lett.*, *23*, 2397–2400, 1996.

Rinsland, C. P., N. B. Jones, B. J. Connor, J. A. Logan, N. S. Pougatchev, A. Goldman, F. J. Murcray, T. M. Stephen, A. S. Pine, R. Zander, E. Mahieu, and P. Demoulin, Northern and southern hemisphere ground-based measurements of tropospheric carbon monoxide and ethane, *J. Geophys. Res.*, *103*, 28,197–28,217, 1998.

Rinsland, C. P., A. Goldman, B. J. Connor, T. M. Stephen, N. B. Jones, S. W. Wood, F. J. Murcray, S. J. David, R. D. Blatherwick, R. Zander, E. Mahieu, and P. Demoulin, Correlation relationships of stratospheric molecular constituents from high spectral resolution, ground-based infrared solar absorption spectra, *J. Geophys. Res.*, *105*, 14,637–14,652, 2000.

Rinsland, C. P., A. Goldman, R. Zander, and E. Mahieu, Enhanced tropospheric HCN columns above Kitt Peak during the 1982–1983 and 1997–1998 El Niño warm phases, *J. Quant. Spectrosc. Radiat. Transfer*, *69*, 3–8, 2001a.

Rinsland, C. P., A. Meier, D. W. T. Griffith, and L. S. Chiou, Ground-based measurements of tropospheric CO, C_2H_6, and HCN from Australia at 34°S latitude, *J. Geophys. Res.*, *106*, 20,913–20,924, 2001b.

Rinsland, C. P., E. Mahieu, R. Zander, A. Goldman, P. Demoulin, and L. S. Chiou, SF_6 ground-based infrared total columns: Long-term trends, pollution events, and a search for SF_5CF_3 in infrared ground-based solar spectra, *J. Quant. Spectrosc. Radiat. Transfer*, in press, 2003.

Rodgers, C. D., Retrieval of atmospheric temperature and composition from remote measurements of thermal radiation, *Rev. Geophys.*, *14*, 609–624, 1976.

Rodgers, C. D., Characterization and error analysis of profiles retrieved from remote sounding measurements, *J. Geophys. Res.*, *95*, 5587–5595, 1990.

Rodriguez, J. M., M. K. W. Ko, and N. D. Sze, Role of heterogeneous conversion of N_2O_5 on sulphate aerosols in global ozone losses, *Nature*, *352*, 134–137, 1991.

Rothman, L. S., et al., The HITRAN molecular spectroscopic database and HAWKS (HITRAN Atmospheric Workstation): 1996 edition, *J. Quant. Spectrosc. Radiat. Transfer*, *60*, 665–710, 1998.

Russell, J. M., III, C. B. Farmer, C. P. Rinsland, R. Zander, L. Froidevaux, G. C. Toon, B. Gao, J. Shaw, and M. Gunson, Measurements of odd nitrogen compounds in the stratosphere by the ATMOS experiment on Spacelab 3, *J. Geophys. Res.*, *93*, 1718–1736, 1988.

Sander, S. P., et al., Chemical kinetics and photochemical data for use in stratospheric modeling, Supplement to evaluation 12: Update of key reactions, Evaluation Number 13, *JPL Publ. 00-03*, 278 pp., 2000.

Sen, B., G. C. Toon, G. B. Ostermann, J. F. Blavier, and J. J. Margitan, Measurements of reactive nitrogen in the stratosphere, *J. Geophys. Res.*, *103*, 3571–3585, 1998.

Shia, R. L., M. K. W. Ko, D. K. Weisenstein, C. Scott, and J. Rodriguez, Transport between the tropical and mid-latitude lower stratosphere: Implications for ozone response to high-speed civil transport emissions, *J. Geophys. Res.*, *103*, 25,435–25,446, 1998.

Tolbert, M. A., M. J. Rossi, and D. M. Golden, Heterogeneous interactions of chlorine nitrate, hydrogen chloride, and nitric acid with sulfuric acid surfaces at stratospheric temperatures, *Geophys. Res. Lett.*, *15*, 847–850, 1988.

Toon, G. C., C. B. Farmer, and R. H. Norton, Detection of stratospheric N_2O_5 by infrared remote sounding, *Nature*, *319*, 570–571, 1986.

Toth, R. A., L. R. Brown, E. A. Cohen, G. C. Toon, and B. Sen, HNO_3 measurements from 850 to 921 cm^{-1}, poster presented in Mid- and Near IR Session of the Workshop on Laboratory Spectroscopy Needs for Atmospheric Sensing, Jet. Propul. Lab., San Diego, Calif., 22 –26 Oct. 2001.

Van Allen, R., F. J. Murcray, T. M. Stephen, and R. D. Blatherwick, Long-term trends in trace gases above Mauna Loa, in *Climate Monitoring and Diagnostics Laboratory, Summary Report 26, 2000–2001*, edited by D. B. King et al., pp. 161–165, U.S. Dep. of Commer., Natl. Oceanic and Atmos. Admin., Environ. Res. Lab., Boulder, Colo., 2002.

Weisenstein, D. K., G. K. Yue, M. K. W. Ko, N.-D. Sze, J. M. Rodriguez, and C. J. Scott, A two-dimensional model of sulfur species and aerosols, *J. Geophys. Res.*, *102*, 13,019–13,035, 1997.

Weisenstein, D. K., M. K. W. Ko, I. G. Dyominov, G. Pitari, L. Ricciardulli, G. Visconti, and S. Bekki, The effect of sulfur emissions from HSCT aircraft: A 2-D model intercomparison, *J. Geophys. Res.*, *103*, 1527–1547, 1998.

World Meteorological Organization (WMO), Scientific assessment of ozone depletion: 1998, *Rep. 44*, 650 pp., Global Ozone Res. and Monit. Proj., Geneva, 1999.

World Meteorological Organization (WMO), Scientific Assessment of ozone depletion: 2002, *Rep. 47*, Global Ozone Res. and Monit. Proj., Geneva, 2003.

Yue, G. K., A new approach to retrieval of aerosol size distributions and integrated properties from SAGE II aerosol extinction spectra, *J. Geophys. Res.*, *104*, 27,491–27,506, 1999.

Zander, R., P. Demoulin, E. Mahieu, L. Delbouille, G. Roland, F. Mélen, C. Servais, M. De Mazière, and M. Van Roozendael, An overview of NDSC-related activities at the Jungfraujoch through high-resolution infrared solar observations, in *Atmospheric Ozone: Proceedings of the XVIII Quadrennial Ozone Symposium, L'Aquila, Italy, September 12–21, 1996*, edited by R. D. Bojkov and G. Visconti, pp. 1005–1008, Edigrafital, Teramo, Italy, 1998.

L. S. Chiou, Science Applications International Corporation, One Enterprise Parkway, Hampton, VA 23666-1498, USA. (l.s.chiou@larc.nasa.gov)

P. Demoulin, E. Mahieu, and R. Zander, Institute of Astrophysics and Geophysics, University of Liège, 17 Allée du 6 Août, 4000 Liège, Belgium. (Emmanuel.Mahieu@ulg.ac.be; R.Zander@ulg.ac.be; demoulin@astro.ulg.ac.be)

C. J. Scott and D. K. Weisenstein, Atmospheric and Environmental Research, Inc., 131 Hartwell Ave., Lexington, MA 02421-3126, USA. (scott@aer.com; dweisens@aer.com)

M. K. W. Ko and C. P. Rinsland, Atmospheric Sciences Competency, NASA Langley Research Center, 21 Langley Blvd., Mail Stop 402, Hampton, VA 23681-2199, USA. (m.k.ko@larc.nasa.gov; c.p.rinsland@larc.nasa.gov)